ASEAN Engineering Journal

Full Paper

REMOVAL OF TETRACYCLINE IN AQUEOUS SOLUTION USING KOH TREATED DIATOMACEOUS EARTH

Sarawut Sinpichai[a], Ratanaporn Yuangsawad[b], Duangkamol Na-Ranong[a]*

[a]Department of Chemical Engineering, School of Engineering, King Mongkut's Institute of Technology Ladkrabang, Bangkok 10520, Thailand
[b]Division of Chemical Engineering, Faculty of Engineering, Rajamangala University of Technology Krungthep, 2 Nanglinchee, Sathorn, Bangkok, 10120, Thailand

Article history
Received
05 January 2024
Received in revised form
01 May 2024
Accepted
23 May 2024
Published online
30 November 2024

*Corresponding author:
duangkamol.na@kmitl.ac.th

Graphical abstract

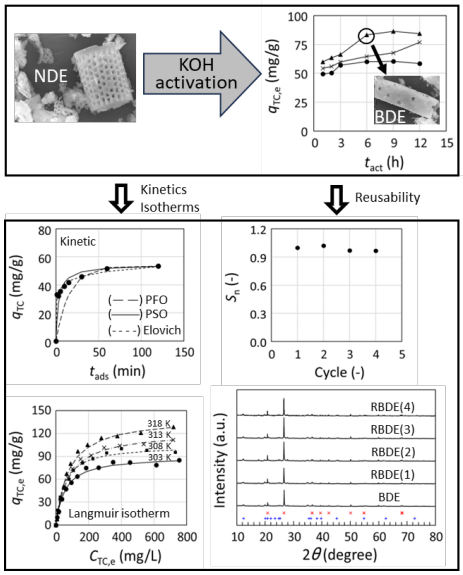

Abstract

Contamination of tetracycline group antibiotics (TC) has become more serious environmental problem. Diatomaceous earth (DE) activated by KOH impregnation is one of feasible adsorbents applied to TC removal. This paper aims to find the suitable condition for KOH activation, to investigate the adsorption behavior of DE activated at this condition (BDE), to regenerate the spent BDE (SBDE), as well as, to evaluate reusability of the regenerated BDE (RBDE). By comparing adsorption capacities ($q_{TC,e}$) of DEs activated under various conditions (1 – 12 h and 333 – 353 K), the most suitable condition was determined as 6 h and 353 K. Linear regression analysis of kinetics and isotherm experimental data revealed that pseudo-second-order model gave the best fit with the kinetics data, comparing with pseudo-first-order and Elovich models and Langmuir isotherm model fitted with the isotherm data better than Freundlich model. Furthermore, SBDE was successfully regenerated using the procedure similar to the activation step but under milder conditions; impregnation of SBDE in 0.1 M KOH solution at 303 K for 1 h. Although $q_{TC,e}$ of RBDE dropped around 24% of the original value after the first regeneration, it was nearly constant even after 4 cycles of adsorption-regeneration experiment.

Keywords: adsorption, diatomaceous earth, isotherm, kinetics, tetracycline, regeneration

1.0 INTRODUCTION

Tetracycline group antibiotics (TC) are widely detected in many wastewater treatment plants [1] and they are also runoff from livestock operations [2]. The concentration of TC in wastewater varies depending on their sources. For examples, the values up to 500 mg/L have been reported for the effluents from hospital and pharmaceutical manufacturing wastewater [3] or even as low as 72,156.9 ng/L in the effluent from pig farms [4]. Since the contamination of TC in the environment leads to drug resistance, it is crucial to prevent the wider spread of TC in the environment. Several techniques such as oxidation, filtration, and adsorption [1, 4, 5, 6] have been investigated for TC removal and reported in literature. Adsorption with highly efficient adsorbent is one of the promising alternatives because its operation is simple and it requires low costs of installation and operation.

Diatomaceous earth (DE) is a naturally occurring sedimentary rock composed of fossilized diatoms, hard-shelled algae whose skeletons are primarily made of silica derived from silicon dioxide (SiO_2). Alongside diatomaceous skeletons, DE also contains clay minerals, quartz, and small proportion of organic matter [7]. Several chemical substances, including SiO_2, Al_2O_3, Fe_2O_3 and many other minor components, present in DE and the composition widely varies depending on the origin [8]. As a naturally available, abundant and cheap porous material, DE has been widely applied to many commercial scale applications including in adsorption processes to remove trace of impurities in beverage, edible oil and so on. However, disposal of the spent DE adsorbent has been the main disadvantage of its application. To solve this problem, it is necessary to prepare

high adsorption efficiency of fresh DE and to reasonably reuse the spent DE before being disposed.

In general, natural diatomaceous earth (NDE) must be thermally or chemically processed to get rid of impurities and to enhance adsorption efficiency. During the treatments, morphology and chemical and physical properties of NDE are modified and hence the improve of affinity to adsorbates could be improved [9, 10, 11].

In the previous work [12], strong acid (H_2SO_4) and strong base (KOH) solutions were used in chemical treatment in order to enhance the efficiency of a local natural diatomaceous earth (NDE) in TC removal. It was found that TC adsorption efficiency could be enhanced through the alkaline treatment, however, the acid treatment exhibited some negative effects on the efficiency. Furthermore, only activation temperature (T_{act}) and activation time (t_{act}) of this basic treatment significantly influenced the adsorption performance of the obtained basic treated diatomaceous earth. Therefore, this present work was conducted in order to determine the suitable condition to achieve highly efficient activated DE for TC removal application. After the most suitable condition was found, the DE activated at this condition, namely as BDE, was used for further investigation in aspects of kinetics and isotherm behaviors as well as the reusability and stability.

2.0 METHODOLOGY

2.1 Materials and Chemicals

Natural diatomaceous earth (NDE) originated from a local clay factory in the northern of Thailand was used to prepare the activated DE. Potassium hydroxide (KOH, AR grade, 85%, Univar) was used as an activating agent. Tetracycline hydrochloride (AR grade, 99%, Vesco Pharmaceutical Co., Ltd.) was used to prepare the model solution of TC contaminated wastewater.

2.2 Activation of Diatomaceous Earth

Activation of NDE was performed with the same procedure as reported in the previous work [12]. Firstly, NDE (2 g) was impregnated in KOH aqueous solution (20 mL) in a glass bottle. Then, the mixture was shaken in an orbital shaker at the activation temperature (T_{act}). After the activation time (t_{act}) was reached, the sample was cooled and washed several times with distilled water until pH of the washed water was 7. In order to determine the suitable condition for preparation of highly effective activated diatomaceous earth, the temperature (T_{act}) and the time (t_{act}) in activation were varied (T_{act} = 333 – 353 K and t_{act} = 1 – 12 h) since it was found that only these two parameters significantly affected the efficiency of the obtained adsorbent. Other two insignificant activation parameters were fixed based on the result previously reported [12]: relative amount of NDE and KOH solution (*NDE-to-Sol*) and concentration of KOH solution (C_{KOH}) were fixed at 0.1 g/ml and 3 M, respectively. The prepared base-activated diatomaceous earth was named as DE-*X*-*Y*, where *X* and *Y* represented T_{act} and t_{act}, respectively.

2.3 Characterization of Adsorbent

Composition, porous property, morphology, crystallinity and surface functional groups of the adsorbent were observed using an X-ray Fluorescence Spectrometer (JEOL; JSX3400R), an adsorption-desorption isotherm of nitrogen at 77 K (TriStar II Plus 3.02; Micromeritics), a scanning electron microscope (LSM-5410LV; JEOL), an X-ray diffractometer (Empyrean Series 3; Malvern PANalytical®) and a Fourier Transform-Infrared Spectrometer (ATR Shimadzu), respectively.

2.4 Adsorption Experiment

To evaluate the performance of activated diatomaceous earth activated at various conditions, adsorption experiment was conducted with the same procedure as described in the previous work [12] where adsorption was tested at room temperature (T = 303 K) with initial concentration ($C_{TC,0}$) of 400 mg/L, adsorbent dosage of 2 g/L and time of 6 h.

Concentrations of TC in the samples taken before and after adsorption experiment were measured using a UV-Visible spectrophotometer (Evolution 210, Thermo Fischer Scientific). Two major peaks were observed at 275 and 355 nm in the full scan spectrum. However, the measurement was performed at 355 nm where the maximum absorption intensity was observed. The correlation factor (R^2) of the calibration curves were as high as 0.9999.

Adsorption capacity (q_{TC}) was calculated according to Eq. (1)

$$q_{TC} = (C_{TC,0} - C_{TC})V/m \quad (1)$$

where $C_{TC,0}$ and C_{TC} are concentrations of TC (mg/L) at the initial and at the specific time of adsorption, respectively, V is volume of TC solution (L) and m is mass of adsorbent (g).

The most suitable activation condition was selected and only the diatomaceous earth activated at this condition, named as BDE, was used for further investigations of isotherm, kinetics and reusability.

In isotherm and kinetic experiments, adsorption temperature was varied in range of 303 – 318 K. $C_{TC,0}$ was varied from 25 to 960 mg/L for isotherm investigation while it was set at 200 mg/L for kinetics investigation.

2.5 Regeneration of BDE

To test the reusability of BDE, regeneration of the spent BDE (SBDE) was performed at various conditions and the suitable regeneration condition was determined. Consequently, $q_{TC,e}$ was measured after several cycles of adsorption-regeneration to evaluate the stability of BDE.

The adsorption experiment was conducted at 250 mL, 303 K and 6 h. After that, SBDE was separated from the adsorption mixture by vacuum filtration and the collected SBDE was dried in an oven at 383 K for 6 h. To regenerate SBDE, the dried SBDE was impregnated in KOH solution with the procedure similar to NDE activation process. After the impregnation, the regenerated BDE (RBDE) was washed, separated, dried and reused for the next cycle of adsorption test.

To determine the suitable condition for SBDE regeneration, C_{KOH} was varied in the range of 0.01 – 1 M, temperature (T_{regen}) was varied as 303 and 323 K while *SBDE-to-*

Sol and impregnation time were constant at 0.01 g/mL and 1 h, respectively.

To evaluate the stability of RBDE (S_n) after several cycles of adsorption-regeneration, the adsorption capacities of RBDE after *n* cycles was compared with the one after the first cycle, calculated according to Eq. (2).

$$S_n = q_{TC,\,RBDE(n)} \,/\, q_{TC,\,RBDE(1)} \qquad (2)$$

2.6 Kinetics and Isotherm Models

Three general models, pseudo-first order (PFO), pseudo-second order (PSO) and Elovich (EV) were applied to interpretation of the kinetics data. As for the analysis of the isotherm data, two conventional models, Langmuir and Freundlich were considered.

3.0 RESULTS AND DISCUSSION

3.1 Preparation of Highly Efficient BDE

Figure 1 shows adsorption capacity (q_{TC}) of diatomaceous earth activated at various activation conditions (t_{act} and T_{act}). In this range of t_{act}, increase in T_{act} significantly enhances q_{TC} of the obtained DE-*X*-*Y*s. On the other hand, q_{TC} increases with t_{act} only when t_{act} increases from 1 to 6 h while beyond this activation time q_{TC} seems to plateau or even slightly drops, except at T_{act} of 343 K. Based on this result, 353 K was selected as the most effective T_{act}. Although DE-*353-9* showed the highest efficiency, the condition of 353 K and 6 h was selected as the most suitable activation condition. This is because the shorten t_{act} from 9 to 6 h, corresponding to 33.33% reduction of energy consumption, resulted in only 3.27 % decrease of adsorption efficiency; $q_{TC,\,DE\text{-}353\text{-}9}$ = 86.31 mg/g while $q_{TC,\,DE\text{-}353\text{-}6}$ = 83.49 mg/g. Consequently, DE activated at 353 K for 6 h, namely as BDE, was used for further investigation.

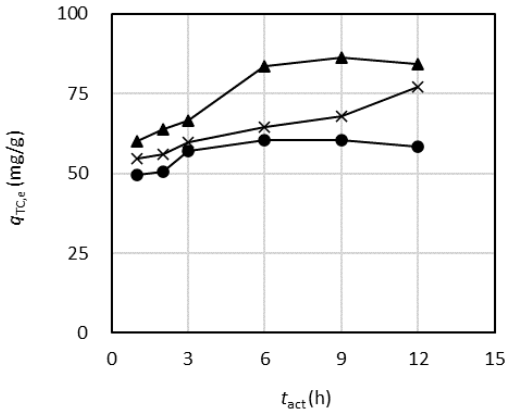

Figure 1 Effects of activation conditions on performance of DE-*X*-*Y* in TC adsorption. Activation temperature at (●) 333, (x) 343 and (▲) 353 K.

3.2 Characterizations of NDE and BDE

As summarized in Table 1, NDE and BDE mainly consisted of SiO_2, Al_2O_3 and Fe_2O_3. SiO_2 content was largely reduced from 71.9% in NDE to 55.1% in BDE while other components were slightly increased. This result indicated that the KOH treatment was effective in dissolution of SiO_2, as reported in literature [9, 13].

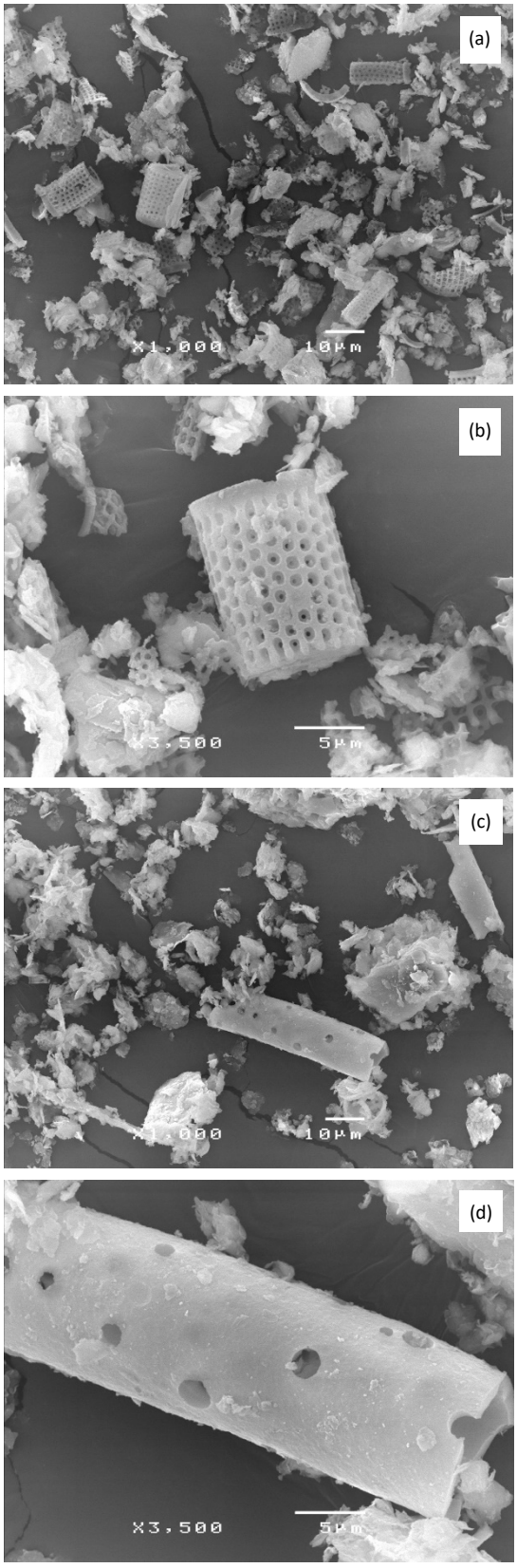

Figure 2 SEM images of (a, b) NDE and (c, d) BDE

Figures 2(a) and (b) demonstrate that the frustules existed in NDE as small fragments, short and long rod-like structures and

Table 1 Composition of NDE and BDE from XRF analysis

Property	Unit	NDE*	BDE
SiO_2	wt%	71.90	55.10
Al_2O_3	wt%	11.70	20.60
Fe_2O_3	wt%	6.28	10.40
K_2O	wt%	1.61	6.00
MgO	wt%	0.41	0.96
SSA_{BET}	m^2/g	25.39	27.18
V_T	cm^3/g	0.03	0.10
d_P	nm	4.69	14.88

*as reported in Ref. [12]

these frustules contained many small pores which were in uniform circular shape (diameter around 1 µm) and well order arrangement. After the KOH treatment, the morphology was obviously changed. As shown in Figure 2(c) and (d), no small pores were observed in the small fragments and less pores existed in the rod-like structures of BDE. This pore closure was considered as a result of the etching reaction by KOH during the activation.

As illustrated in Figure 3, NDE and BDE and SBDE have the same XRD diffraction patterns. The two peaks with strong intensity at 20.8 and 26.6° reveal the existence of quartz and the tiny peak at 12.37° reveal the existence of kaolinite. The similar characteristic patterns of NDE and BDE indicated that the KOH treatment at this condition only modified the amorphous phase and insignificantly affected the crystallinity of the adsorbent. No change in the crystallinity of adsorbent was observed after the adsorption experiment.

A series of FT-IR spectra of NDE, BDE and SBDE illustrated in Figure 4 also confirmed the modification of amorphous phase with insignificant effect on the crystallite silicate structure of the adsorbent caused by the KOH activation. The spectrum of NDE shows the strong and broad band around 1060 – 1090 cm^{-1} attributed to Si-O-Si asymmetric bond stretching vibration, the group of small peaks at 3695 and 3626 cm^{-1} attributed to OH unassociated silanol group and two small peaks at 914 and 800 cm^{-1} attributed to Si-OH stretching vibration and Si-O-Si symmetric bond stretching vibration, respectively [14]. The small peaks appear at 694 and 540 cm^{-1} are assigned to O-Si-O bending and Si-O-Al in kaolinite structure, respectively [15]. Comparison of BDE spectrum with NDE spectrum reveals that after NDE was activated to BDE, the strong and broad peak around 1060 – 1090 cm^{-1} became sharper and slightly shifted to 1002 cm^{-1}, which is important characteristic of FT-IR spectrum of amorphous phase silica, implying the change from crystalline to amorphous phase of silica due to the KOH activation. In the

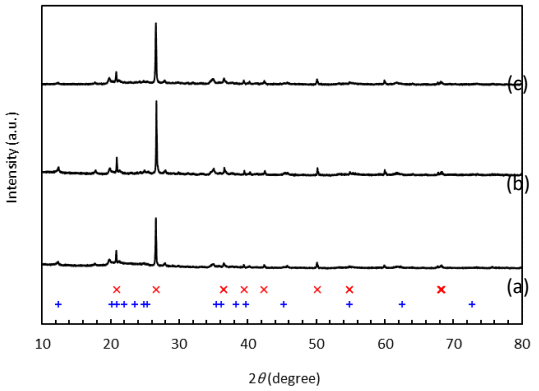

Figure 3 XRD patterns of (a) NDE, (b) BDE and (c) SBDE; standard patterns of (x) silica and (+) kaolinite

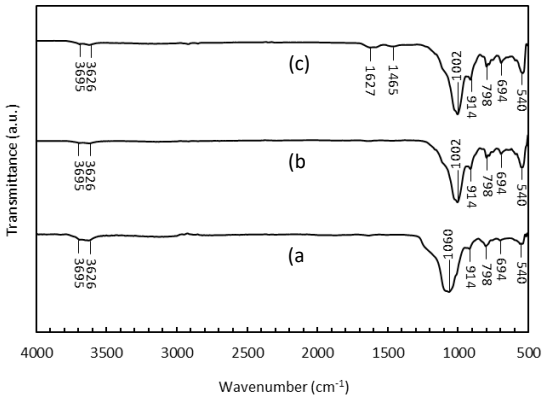

Figure 4 FTIR spectra of (a) NDE, (b) BDE, and (c) SBDE.

Table 2 Linear form equations and parameters of each kinetics and isotherm model

Model			Parameter and Unit		Adsorption Temperature (K) 303	308	313	318
Kinetics	PFO	$\ln\left(\frac{q_{TC,e}}{q_{TC,e}-q_{TC}}\right)=k_1 t_{ads}$	q_e	mg/g	60.40	53.54	53.37	56.14
			k_1	1/min	0.0640	0.0634	0.0649	0.0440
			R^2	-	0.8530	0.9616	0.9063	0.4664
	PSO	$\frac{t_{ads}}{q_{TC}}=\frac{1}{k_2 q_{TC,e}^2}+\frac{t_{ads}}{q_{TC,e}}$	q_e	mg/g	60.14	54.53	53.66	56.57
			k_2	g/mg/min	0.0055	0.0058	0.0080	0.0106
			R^2	-	0.9945	0.9985	0.9987	0.9996
	Elovich	$q_{TC}=\left(\frac{1}{\beta}\right)\ln(\alpha\beta)+\left(\frac{1}{\beta}\right)\ln(t_{ads})$	a	mg/g/min	24958	1743	1895	3686
			β	g/mg	0.2334	0.2012	0.1969	0.1949
			R^2	-	0.9460	0.9308	0.9722	0.9669
Isotherm	Langmiur	$\frac{C_{TC,e}}{q_{TC,e}}=\frac{1}{q_L k_L}+\frac{C_{TC,e}}{q_L}$	q_L	mg/g	90.20	104.58	123.61	142.25
			k_L	L/mg	0.0187	0.0216	0.131	0.129
			R^2	-	0.9964	0.9968	0.9988	0.9981
	Freundlich	$\ln(q_{TC,e})=\ln(k_F)+\frac{1}{n_F}\ln(C_e)$	k_F	mg/L	6.036	7.168	4.859	4.937
			n_F	-	2.2631	2.2440	1.8882	1.8042
			R^2	-	0.9025	0.9136	0.9080	0.9065

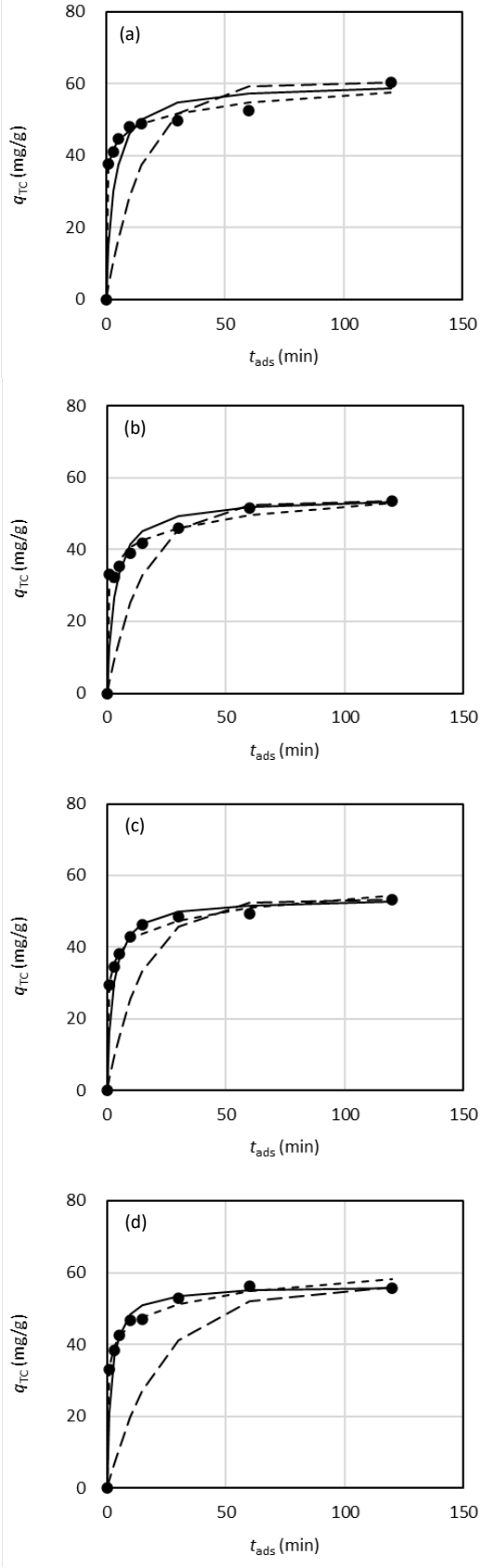

Figure 5 Kinetics of TC adsorption on BDE at (a) 303, (b) 308, (c) 313 and (d) 318 K; ($C_{TC,0}$ = 200 mg/L and adsorbent dosage = 2 g/L); symbol is experimental data and lines present calculated results based on (— —) PFO, (——) PSO, and (- - - -) Elovich models.

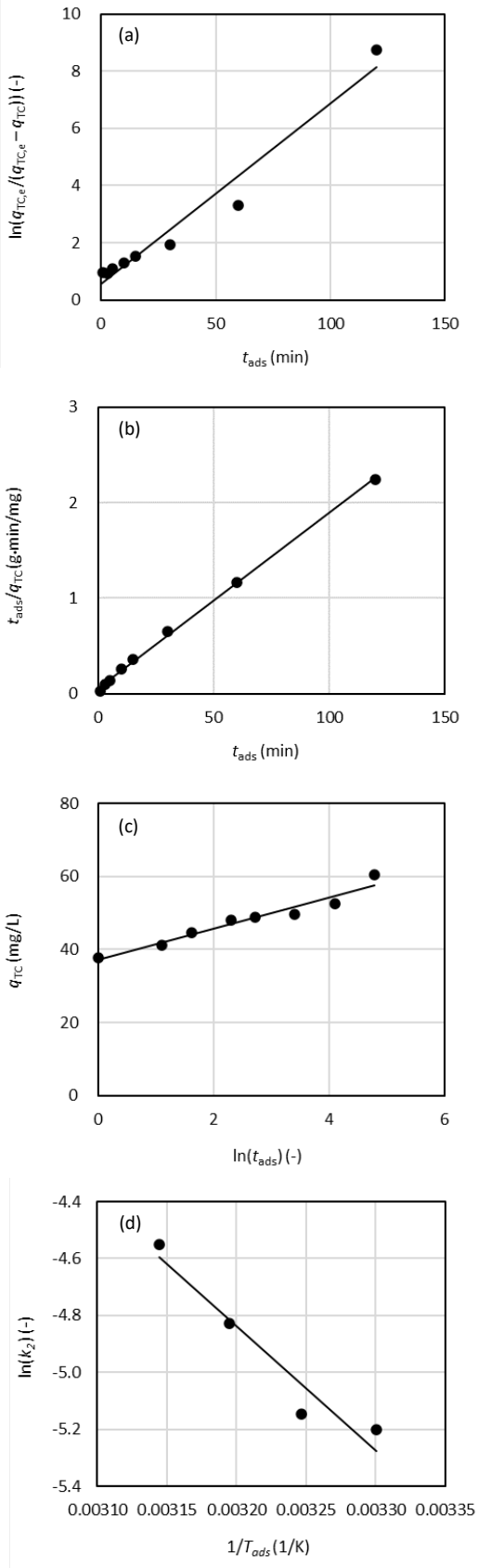

Figure 6 Linear plots of kinetics data at 308 K based on (a) PFO, (b) PSO, (c) Elovich models, and (d) Arrhenius plot of k_2 calculated using PSO model

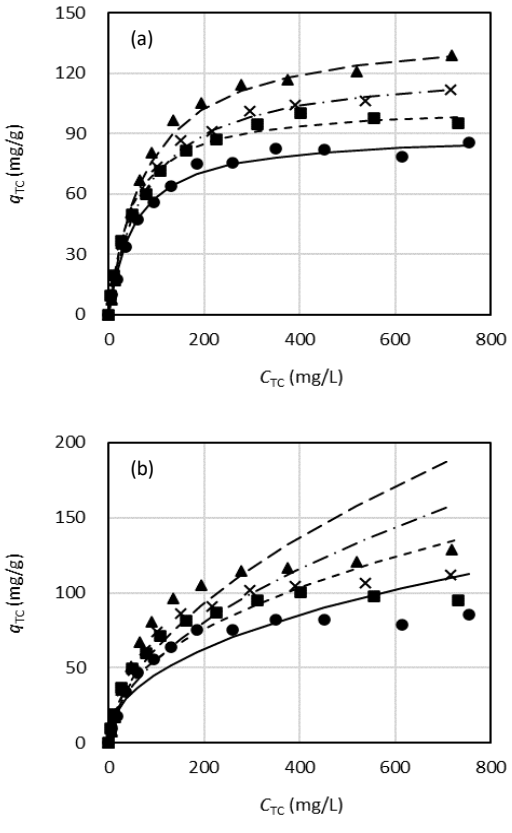

Figure 7 Fits of (a) Langmuir and (b) Freundlich isotherm models with experimental data at (●, ——) 303, (■, - - - -) 308, (×, — · —) 313, and (▲, — — —) 318 K: adsorbent dosage = 2 g/L, t_{ads} = 6 h; symbol and line represent experimental data and calculated results, respectively.

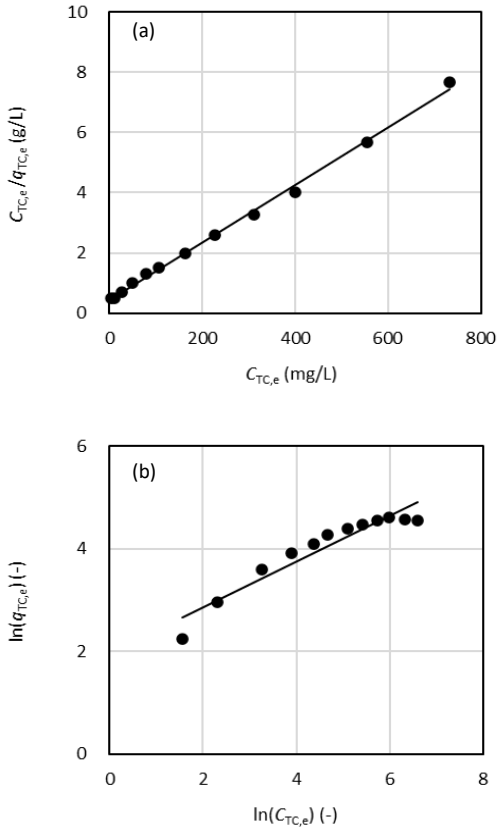

Figure 8 Fits of (a) Langmuir and (b) Freundlich isotherm models with experimental data at 308 K, adsorbent dosage = 2 g/L, t_{ads} = 6 h; (●) experimental data, (——) calculated result.

spectrum of SBDE, additional to the characteristic bands of silicate structure in ranges of 500 – 1400 and 3626 – 3695 cm^{-1}, the small broad peaks around 1627 cm^{-1} assigned to C=C stretching and around 1465 cm^{-1} assigned to C-H bending [16] appear. This result indicates the existence of TC molecules on SBDE sample.

3.3 Adsorption Kinetics

Time dependences of q_{TC} at various adsorption temperatures (T_{ads}) are demonstrated as the symbol-plot in Figure 5. The rate of TC adsorption rapidly occurred in the induction period and gradually decreased after 15 min. This behavior is expected as general adsorption because initially there are abundant vacant sites available for molecules of adsorbate to be adsorbed and the concentration of adsorbate in the solution is also high, whereas in the later period the number of vacant sites and the concentration of adsorbate becomes smaller. It should be noted that it was confirmed by the separated experimental runs that the adsorption in this temperature range reached the equilibrium within 6 h.

Table 2 presents the linear equations and the corresponding results of linear regression analysis according to PFO, PSO and Elovich models including correlation factor (R^2) and the evaluated kinetics parameters. As an example, the linear plots according to PFO, PSO and Elovich models obtained at 308 K are illustrated in Figure 6 (a) – (c). The plots clearly show that the goodness of fit of the model were in the order of PSO > Elovich > PFO and the line-plot in Figure 5 also confirmed that PSO was the most suitable model to describe the kinetics of TC adsorption on BDE. At other T_{ads}, the similar trends were also observed. Furthermore, the activation energy of TC adsorption evaluated from Arrhenius plot of PSO model, ln(k_2) vs 1/T_{ads} in Figure 6 (d), was 36.57 kJ/mol/K.

3.4 Adsorption Isotherm

Isotherm plot, illustrated as symbols in Figure 7, reveals that $q_{TC,\,e}$ steeply increases with $C_{TC,\,e}$ in low concentration region and gradually reaches the saturation at high concentration. The saturation is evidently observed around 80 mg/g at 303 K and around 100 mg/g at 308 K while the saturation just nearly reaches at the temperature higher than 308 K. The linear plots according to Langmuir and Freundlich isotherm models, as illustrated in Figure 8, and the values of R^2 obtained from linear regression analysis, listed in Table 2, suggested that Langmuir model gave the fit with experimental result better than Freundlich model. This was also confirmed by the plots in Figure 7, where a strong resemblance between the calculated result and the experimental data was found only in the case of Langmuir isotherm model. This result implied that TC adsorbed on the surface of BDE as monolayer without interactions between the adsorbed TC. In addition, the increase in saturation capacity of TC adsorption (qL) with Tads was consistent well with the

Table 3. Comparison of TC adsorption capacities; Q_{max} is the maximum adsorption capacity calculated according to Langmuir isotherm model.

Adsorbents	Adsorption Conditions	Q_{max} (mg/g)	Ref.
BDE	2 g/L, 6 h, 318 K	142.25	This work
Amino and amino-Fe^{3+} functionalized mesoporous silica	1 g/L, 24 h, 298 K, pH 5	90.77	[17]
Palygorskite supported Cu_2O-TiO_2	1 g/L, 1 h, 293 K, pH 8.7	113.6	[18]
Chitosan modified bentonite	5 g/L, 0.5 h, 313 K	121.36	[19]
Clay mineral montmorillonite	0.5 g/L, 6 h, 298 K	227.27	[20]

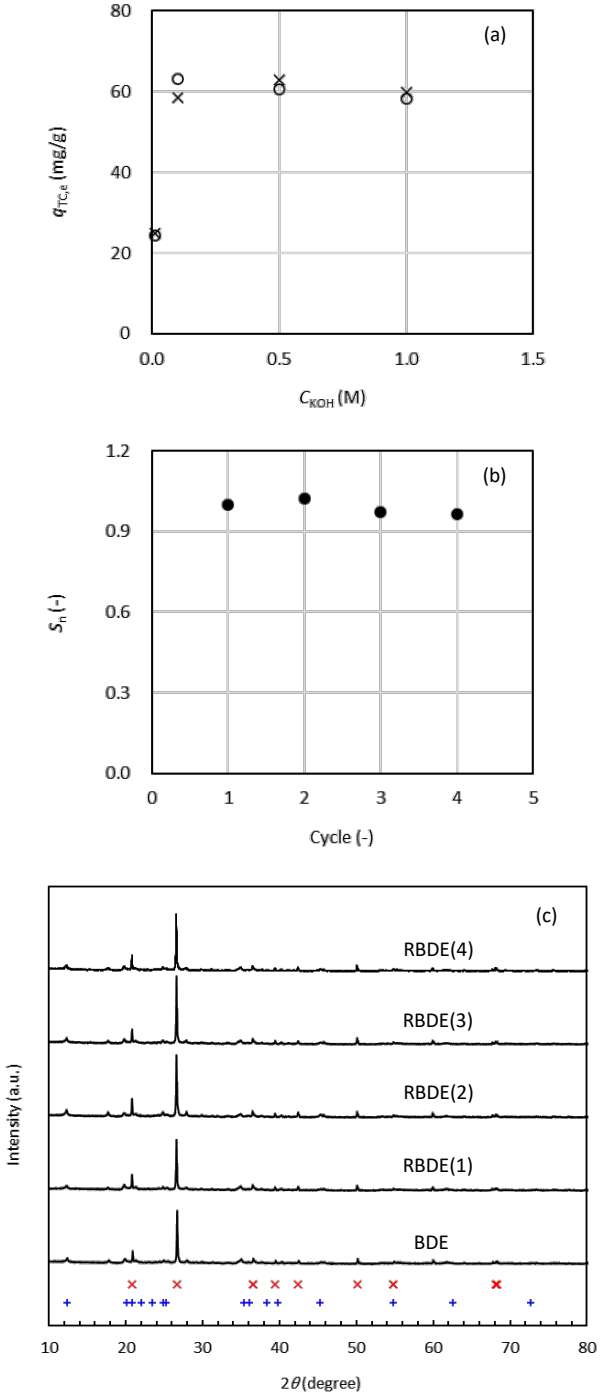

Figure 9 (a) Regeneration of SBDE at (○) 303 and (×) 323 K, (b) Reproducibility of BDE efficience after several adsorption-regeneration cycles, (c) XRD patterns of RBDEs with the standard patterns of (x) silica and (+) Kaolinite and number in parenthesis represents the number of regeneration.

determined k_L at various T_{ads} (in Table 2), implying endothermic behavior of this adsorption process.

Table 3 shows the comparison of the maximum adsorption capacity (Q_{max}) of BDE with other adsorbents in literature; BDE should be considered as one of the promising alternatives for TC removal.

3.5 Reusability: Regeneration and Stability

Regeneration of SBDE should be considered since it is a key to cost-effective and environmentally sustainable solution for large scale wastewater treatment plant. In this study, the regeneration of SBDE was tested using KOH impregnation similar to the activation method but under the milder conditions, C_{KOH} = 0.01 – 1 M and regeneration temperatures (T_{regen}) of 303 and 323 K.

The results in Figure 9 (a) reveals that SBDE was effectively regenerated when C_{KOH} was as high as 0.1 M and the increase in C_{KOH}, even to 10 times (1 M), slightly affected the efficient of the regeneration. On the other hand, the increase in T_{regen} from 303 to 323 K negligibly influenced the efficient of the regeneration. Therefore, the regeneration at C_{KOH} of 0.1 M and T_{regen} of 303 K, giving q_{TC} = 63.07 mg/g, was performed for further evaluation of reproducibility of adsorption performance after several adsorption-regeneration cycles. It was found that the adsorption capacity of RBDE(1) was about 75.5 % of that of BDE ($q_{TC,\ RBDE(1)}$ = $0.755q_{TC,\ BDE}$). However, as illustrated in Figure 9 (b), this adsorption capacity was constantly maintained up to 4 times of the reuse; S_n varied in quite narrow range (0.97 – 1.02). Figure 9 (c) reveals that the XRD pattern of BDE and RBDEs are similar, implying that the crystalline structure of RBDEs were not affected by the KOH treatment during the regeneration.

4.0 CONCLUSION

In this study, adsorption performance of diatomaceous earth activated by KOH impregnation under various conditions (1 – 12 h and 333 – 353 K) were comparatively measured and the most suitable condition of the activation was determined as 6 h and 353 K. Characterization of diatomaceous earth before and after activation, NDE and BDE, suggested that KOH activation resulted in dissolution and leaching of amorphous phase silica rather than crystalline one. Linear regression analysis revealed that the goodness of fit of kinetics models was in the order of pseudo-second-order (R^2 = 0.9945 – 0.9996) > Elovich (R^2 = 0.9308 – 0.9722) > pseudo-first-order (R^2 = 0.4664 – 0.9616) and the activation energy this adsorption was 36.57 kJ/mol/K. As for isotherm behavior, Langmuir model fitted with experimental data much better than Freundlich model, indicating monolayer adsorption of TC molecules on homogeneous sites of BDE and the increase in adsorption equilibrium constant with temperature

also indicated endothermic behavior. Impregnating SBDE in 0.1 M of KOH solution at 303 K for 1 h reasonably reproduced and maintained efficiency of the regenerated BDE in TC removal at least for 4 cycles of adsorption-regeneration experiment.

Acknowledgement

Financial support from Faculty of Engineering, King Mongkut's Institute of Technology Ladkrabang (2564-02-01-014) is gratefully acknowledged. Vesco Pharmaceutical Co., Ltd. is acknowledged for Tetracycline hydrochloride.

Conflicts of Interest

The author(s) declare(s) that there is no conflict of interest regarding the publication of this paper

References

[1] Chiemchaisri, W., Chiemchaisri, C., Hamjinda, N. S., Jeensarut, C., Buranapakdee, P. and Thammalikitkul, V. 2022. Field Investigation of Antibiotic Removal Efficacies in Different Hospital Wastewater Treatment Processes in Thailand. *Emerging Contaminants*. 8: 329–339. DOI: 10.1016/j.emcon.2022.07.002

[2] Javid, A., Mesdaghinia, A., Nasseri, S., Mahvi, A. H., Alimohammadi, M. and Gharibi, H. 2016. Assessment of Tetracycline Contamination in Surface and Groundwater Resources Proximal to Animal Farming Houses in Tehran, Iran. *Journal of Environmental Health Science and Engineering*. 14(4):1-5. DOI:10.1186/s40201-016-0245-z

[3] Ahmadi, M., Motlagh, H. R., Jaafarzadeh, Nematollah., Mostoufi, A., Saeedi, Reza., Barzegar, G. and Jorfi, S. 2017. Enhanced Photocatalytic Degradation of Tetracycline and Real Pharmaceutical Wastewater using MWCNT/TiO_2 Nano-Composite. *Journal of Environmental Management*. 186: 55–63. DOI: 10.1016/j.jenvman.2016.09.088

[4] Suzuki, S., Ogo, M., Takada, H., Seki, K., Mizukawa, K., Kadoya, A., Yokokawa, T., Sugimoto, Y., Takabe, Y. S., Boonla, C., Anomasiri, W. and Sukpanyatham, N. 2021. Contamination of Antibiotics and Sul and Tet(m) Genes in Veterinary Wastewater, River, and Coastal Sea in Thailand. *Science of the Total Environment*. 791: 148423. DOI: 10.1016/j.scitotenv.2021.148423

[5] Crini, G. 2006. Non-Conventional Low-Cost Adsorbents for Dye Removal: A Review. *Bioresource Technology*. 97(9): 1061–1085. DOI: 10.1016/j.biortech.2005.05.001

[6] Gupta, V. K. and Suhas. 2009. Application of Low-Cost Adsorbents for Dye Removal – A Review. *Journal of Environmental Management*. 90(8): 2313–2342. DOI: 10.1016/j.jenvman.2008.11.017

[7] Lutyński, M., Sakiewicz, P. and Lutyńska, S. 2019. Characterization of Diatomaceous Earth and Halloysite Resources of Poland. *Minerals*. 9(11): 670. DOI: 10.3390/min9110670

[8] Pimraksa, K. and Chindaprasirt, P. 2009. Lightweight Bricks Made of Diatomaceous Earth, Lime and Gypsum. *Ceramics International*. 35(1): 471–478. DOI: 10.1016/j.ceramint.2008.01.013

[9] Tsai, W. T., Hsien, K. J. and Lai, C. W. 2004. Chemical Activation of Spent Diatomaceous Earth by Alkaline Etching in the Preparation of Mesoporous Adsorbents. *Industrial & Engineering Chemistry Research*. 43(23): 7513–7520. DOI: 10.1021/ie0400651

[10] Font, A., Soriano, L., Reig, L., Tashima, M. M., Borrachero, M. V., Monzó, J. and Payá, J. 2018. Use of Residual Diatomaceous Earth as a Silica Source in Geopolymer Production. *Materials Letters*. 223: 10–13. DOI: 10.1016/j.matlet.2018.04.010

[11] Ho, C. H., Lo, H. M., Lin, K. L. and Lan, J. Y. 2018. Characteristics of Porous Ceramics Prepared from Sandblasting Waste and Waste Diatomite by Co-sintering Process. *Environmental Progress & Sustainable Energy*. 38(2): 321–328. DOI: 10.1002/ep.12942

[12] Sinpichai, S., Yuangsawad, R. and Ranong, D. N. 2023. Effects of Acid and Alkaline Treatments on Efficiency of Diatomaceous Earth in Removal of Tetracycline in Aqueous Solution. *ASEAN Engineering Journal*. 13(3): 173–179. DOI: 10.11113/aej.v13.20194

[13] Nakashima, Y., Fukushima, M. and Hyuga, H. 2021. Preparation of Porous Diatomite Ceramics by an Alkali Treatment Near Room Temperature. *Journal of the European Ceramic Society*. 41(1): 849–855. DOI: 10.1016/j.jeurceramsoc.2020.08.056

[14] Bertoluzza, A., Fagnano, C., Morelli, M. A., Gottardi, V. and Guglielmi, M. 1982. Raman and Infrared Spectra on Silica Gel Evolving Toward Glass. *Journal of Non-Crystalline Solids*. 48(1): 117–128. DOI: 10.1016/0022-3093(82)90250-2

[15] Chaisena, A. and Rangsriwatananon, K. 2004. Effects of Thermal and Acid Treatments on Some Physico-Chemical Properties of Lampang Diatomite. *Suranaree Journal of Science and Technology*. 11: 289–299.

[16] Trivedi, M. K., Patil, S., Shettigar, H., Bairwa, K. and Jana, S. 2015. Spectroscopic Characterization of Chloramphenicol and Tetracycline: An Impact of Biofield Treatment. *Pharmaceutica Analytica Acta*. 6(7): 395. DOI: 10.4172/2153-2435.1000395

[17] Zhang, Z., Li, H. and Liu, H. 2017. Insight into the Adsorption of Tetracycline onto Amino and Amino-Fe^{3+} Functionalized Mesoporous Silica: Effect of Functionalized Groups. *Journal of Environmental Sciences*. 65: 171–178. DOI: 10.1016/j.jes.2016.10.020

[18] Shi, Y., Yang, Z., Wang, B., An, H., Chen, Z. and Cui, H. 2016. Adsorption and Photocatalytic Degradation of Tetracycline Hydrochloride using a Palygorskite-Supported Cu_2O–TiO_2 Composite. *Applied Clay Science*, 119: 311–320. DOI: 10.1016/j.clay.2015.10.033

[19] Guo, X., Wu, Z., Wang, Z., Lin, F., Li, P. and Liu, J. 2023. Preparation of Chitosan-Modified Bentonite and Its Adsorption Performance on Tetracycline. *ACS Omega*. 8: 19455–19463. DOI: 10.1021/acsomega.3c00745

[20] Shang, J., Huang, M., Zhao, L., He, P., Liu, Y., Pan, H., Cao, S. and Liu, X. 2023. Adsorption Performance and Mechanisms of Tetracycline on Clay Minerals in Estuaries and Nearby Coastal Areas. *ACS Omega*. 9(1): 692–699. DOI: 10.1021/acsomega.3c06478